

# Droplet-shaped waves: causal finite-support analogs of X-shaped waves

Andrei B Utkin

*INOV - Inesc Inovação and ICEMS, Instituto Superior Técnico,  
Technical University of Lisbon, Av. Rovisco Pais, Lisbon 1049-001, Portugal\**

## Abstract

A model of steady-state X-shaped wave generation by a superluminal (supersonic) point-like source infinitely moving along a straight line is extended to a more realistic causal scenario of a source pulse launched at time zero and propagating rectilinearly at constant superluminal speed. In the case of infinitely short ( $\delta$ ) pulse, the new model yields an analytical solution, corresponding to the propagation-invariant X-shaped wave clipped by a droplet-shaped support, which perpetually expands along the propagation and transversal directions, thus tending the droplet-shaped wave to the X-shaped one.

*OCIS codes:* 350.5720, 320.5550, 350.7420, 070.7345, 350.5500, 070.0070

*PACS numbers:* 43.20.Bi, 03.50.De, 41.20.Jb

arXiv:1110.3494v3 [physics.optics] 2 Jan 2013

---

\*Electronic address: andrei.utkin@inov.pt

## I. INTRODUCTION

The early 1970s witnessed the start of the intensive study of radiation emanated by superluminal sources [1–4], which received a new impetus due to possibility of launching propagation-invariant localized waves [5–9], whose fundamental representations and classification schemes are discussed in [10, 11]. Among different types of the localized wave structures, the X-shaped waves are one of the most well-known [12–14]. Recami et al. [15] proposed a toy model of localized X-shaped field generation by an axisymmetric superluminal four-current  $J^{(\alpha)} = (c\rho, 0, 0, j)$ , where  $c$  is the speed of light,  $\rho$  the electric charge density, and  $j$  the only non-zero component of the current density vector  $\mathbf{j}$  in the cylindrical coordinates  $\rho, \varphi, z$ . Considering the inhomogeneous electromagnetic problem for the four-potential in the form  $A^{(\alpha)} = (A^{(0)}, \mathbf{A}) = (A^{(0)}, 0, 0, \psi)$ ,  $A^{(\alpha)}(\tau, \rho, \varphi, z) = A^{(\alpha)}(\rho, \zeta)$ ,  $\alpha = 0, 1, 2, 3$ , where  $\zeta = z - Vt = z - \beta\tau$  is a  $V$ -cone variable, introduced for constant superluminal velocity  $V = c\beta$ , and  $\tau = ct$  the time variable, the investigation was inevitably constrained to the cases that (i) describe a steady-state process that lasts all times from  $-\infty$  to  $\infty$ , (ii) require similar four-current dependence  $J^{(\alpha)}(\tau, \rho, \varphi, z) = J^{(\alpha)}(\rho, \zeta)$ , and (iii) bound the nonzero components of the four-vectors by relations  $j(\rho, \zeta) = c\beta\rho(\rho, \zeta)$  and  $\psi(\rho, \zeta) = \beta A^{(0)}(\rho, \zeta)$  due to, respectively, the continuity equation and the Lorentz gauge.

The problem was solved for the case of the rectilinear motion of a point-like charge using the spectral method (Fourier-Bessel and Fourier transforms with respect to  $\rho$  and  $\zeta$ ), yielding a localized "true X wave" solution

$$\psi(\rho, \zeta) = const \times \frac{\beta}{\sqrt{\zeta^2 - (\beta^2 - 1)\rho^2}}. \quad (1)$$

Being symmetric with respect to time reversal and involving equally the advanced and retarded components, such a model of X wave generation is acausal. Later attempts to remedy this drawback introducing the unilateral conical-wave source [16] and applying the unidirectional decomposition [17, 18] resulted in more realistic models. All these studies, however, do not take into account the temporal constraint of the source motion – even in its weak form that assumes the existence of an initial moment, prior to which neither the source pulse nor the emanated wave can exist.

## II. STATEMENT OF THE PROBLEM

The present work considers wave generation by superluminal charges within the framework of the Riemann-Volterra approach, introducing a direct space-time domain method that, in contrast to constructing the wavefunctions via the Bateman transform [19, 20] or Green's method [18], deals

with the initial value problem that includes, in addition to the inhomogeneous wave equation

$$[\partial_\tau^2 - \rho^{-1}\partial_\rho(\rho\partial_\rho) - \partial_z^2] \psi(\tau, \rho, z) = S(\tau, \rho, z), \quad (2)$$

the time asymmetric initial condition

$$\psi = 0, \quad S = 0 \quad \text{for } \tau < 0, \quad (3)$$

which defines the *arrow of time* and, as will be shown, represents a sufficient condition for existence of a unique causal solution. For the electromagnetic waves, we assume that  $\psi$  and  $S = \mu_0 j$  represent, respectively, the  $z$ -components of the four-potential  $A^{(\alpha)}$  and four-current  $J^{(\alpha)}$  ( $\mu_0$  stands for the magnetic constant). Furthermore, let us get over one singularity, considering, instead of the line  $\delta$ -pulse, a line source of arbitrary shape  $f(\xi) = f(-\zeta) = f(\beta\tau - z)$  propagating with a constant superluminal speed in the positive  $z$ -direction. In view of (2), (3), such a source can be expressed in the form

$$j(\tau, \rho, z) = ce\beta \frac{\delta(\rho)}{2\pi\rho} h(z) h(\beta\tau - z) f(\beta\tau - z), \quad (4)$$

where  $e$  is the elementary charge while  $\delta(\cdot)$  and  $h(\cdot)$  stand for the Dirac delta and Heaviside step functions.

One can easily notice that due to (3) in no case the problem in question can yield a pure localized solution meeting the propagation-invariant condition stated by Lu (Ref. [5], p. 98) as reducibility to the form  $\psi(\tau, \rho, z) = \psi(\rho, \xi)$ . Instead, it provides us with bounded-support, finite-energy wavefunctions (signals) that can serve as real-world, physically admissible approximations of the ideal temporally unbounded localized waves. Borrowing the terminology from the numerical analysis, we may say that the description of a localized propagation-invariant wave by such a signal is convergent if the signal asymptotically approaches the localized wave structure as  $\tau \rightarrow \infty$ .

The continuity equation  $c\partial_\tau \varrho + \partial_z j = 0$  and representation (4) immediately implies that the charge density is uniquely defined by equation

$$\begin{aligned} \varrho(\tau, \rho, z) &= -\frac{1}{c} \int_0^\tau d\tau' \partial_z j = e \frac{\delta(\rho)}{2\pi\rho} \left[ h(z) h(\beta\tau - z) f(\beta\tau - z) \right. \\ &\quad \left. - \beta h(\tau) \delta(z) \int_0^\tau d\tau' f(\beta\tau' - z) \right] = \frac{1}{c\beta} j + (-e) \frac{\delta(\rho)}{2\pi\rho} h(\tau) \delta(z) \int_0^{\beta\tau} d\xi f(\xi), \end{aligned} \quad (5)$$

and the other non-zero component of the four-potential  $A^{(0)}$  – automatically satisfying  $\square A^{(0)} = \mu_0 J^{(0)}$  – can be obtained as a consequence of (2), (3), and (5) from the Lorenz gauge  $\sum_\alpha \partial_\alpha A^{(\alpha)} = 0$  by a simple integration

$$A^{(0)} = - \int_0^\tau d\tau' \partial_z A^{(3)} = - \int_0^\tau d\tau' \partial_z \psi. \quad (6)$$

Here the second term describes accumulation of the opposite charge at the pulse-generation point  $\rho = 0, z = 0$  due to current outflow.

For models concerning the wave emanation by hypothetical superluminal particles, tachyons, such an accumulation can be nulled if we suppose that the generation of a particle is accompanied by generation of an antiparticle (an opposite point-like charge) moving in different direction.

For other models involving more traditional source structures the excessive charge accumulation can be avoided in the long term by considering (bipolar) current pulses for which  $\int_0^\infty d\xi f(\xi)$  is vanishing or, at least, limited (demonstrating, for example, oscillating behavior). One of such embodiments discussed by Ziolkovski et al. [21] and later by Saari [22] involves superluminal sink-source-type fictitious currents [23]. As discussed in [22] with reference to Fig. 1 therein, the simplest and most straightforward implementation of the superluminal wave motion can be achieved with a type of "scissor effect", creating an interference pattern of two (luminal-speed) plane waves whose fronts are inclined with respect to each other. Similar patterns can be created, e.g., at oblique incidence of wavefronts onto locally plane targets (screens). On the cosmic scale, this phenomena is well discussed by astrophysicists (see, e.g., [24]). Remarkably, recent advances in ultraintense laser interaction science enables such huge-scale phenomena to be reproduced in the micrometer scale in the laboratory conditions. Excitation of a source current pulse by an ultra-intense, ultra-short pulsed laser beam, incident at an angle to a thin plasma filament — induced in a medium by another laser beam — is an example (here significant current density can be obtained due the effects akin to the wake-field acceleration while the desired orientation of the macroscopic current along the filament can be asserted by imposing a strong magnetic field; description of pertinent phenomena can be found in [25]).

### III. GENERAL SOLUTION

Separating  $\rho$  by the Fourier-Bessel transform  $\Psi(\tau, s, z) = \int_0^\infty d\rho \rho \psi(\tau, \rho, z) J_0(s\rho)$ , one gets from (2), (3) and (4) a simpler time asymmetric initial value problem for the Klein-Gordon equation

$$(\partial_\tau^2 - \partial_z^2 + s^2) \Psi = \frac{\mu_0}{2\pi} ce\beta h(z) h(\beta\tau - z) f(\beta\tau - z), \quad (7)$$

with the initial condition

$$\Psi = 0 \quad \text{for} \quad \tau < 0. \quad (8)$$

One can easily check by direct enumeration that condition (8) uniquely defines the transition to the (characteristic) variables  $z, \tau \rightarrow \frac{1}{2}(\tau + z), \frac{1}{2}(\tau - z)$  that: (i) transforms the Klein-Gordon equation to

the first canonical form and (ii) results in the geometry of the solution support, the area of  $\Psi \neq 0$ , corresponding to the well-established layout of the Riemann-Volterra method (see, e.g., Fig. 30 in [26] or Fig. 1 in [27]). The *ad hoc* Riemann-Volterra procedure involving known Riemann function  $J_0\left(s\sqrt{(\tau - \tau')^2 - (z - z')^2}\right)$  (see [28] for details) readily provides a unique causal solution [27], which after the inverse transition to the independent variables  $z, \tau$  takes the form

$$\begin{aligned} \psi(\tau, s, z) &= \frac{\mu_0}{4\pi} ce\beta \int_{z-\tau}^{z+\tau} dz' \int_0^{\tau-|z-z'|} d\tau' J_0\left(s\sqrt{(\tau - \tau')^2 - (z - z')^2}\right) \\ &\times h(z') h(\beta\tau' - z') f(\beta\tau' - z'). \end{aligned}$$

Using the inverse Fourier-Bessel transform, the closure equation (see, e.g., [29], p. 691)

$$\int_0^\infty ds s J_0(s\rho) J_0(s\rho') = \frac{1}{\rho} \delta(\rho - \rho')$$

and the representation of the delta function with simple zeros  $\{\tau_i\}$  ([29], p. 87)

$$\delta(g(\tau)) = \sum_i \frac{\delta(\tau - \tau_i)}{|\partial_\tau g(\tau_i)|} \quad (9)$$

(among the two simple zeros, only one lies within the integration limits), we get the solution to the initial space-time domain problem (2), (3) in the form

$$\begin{aligned} \psi(\tau, \rho, z) &= \frac{\mu_0}{4\pi\rho} ce\beta \int_{z-\tau}^{z+\tau} dz' \int_0^{\tau-|z-z'|} d\tau' h(z') \\ &\times h(\beta\tau' - z') f(\beta\tau' - z') \frac{\delta\left(\tau' - \tau + \sqrt{\rho^2 + (z - z')^2}\right)}{\sqrt{\rho^2 + (z - z')^2}}. \end{aligned} \quad (10)$$

As illustrated in Fig. 1,  $\psi$  is defined by integration over the curve segment  $\Gamma_i = \Delta_{\tau z} \cap H_{z'} \cap H_\beta \cap \Gamma$  that is the intersection of: the initial triangle integration area  $\Delta_{\tau z} = \{z - \tau < z' < z + \tau, 0 < \tau' < \tau - |z - z'|\}$ ; the half-plane  $H_\beta = \{\beta\tau' - z' > 0\}$ , the support of the step function  $h(\beta\tau' - z')$ ; the half-plane  $H_{z'} = \{z' > 0\}$ , the support of the step function  $h(z')$ ; and the hyperbola  $\Gamma = \{\tau' - \tau + \sqrt{\rho^2 + (z - z')^2} = 0\}$ , the support of the delta function  $\delta(\tau' - \tau + \sqrt{\rho^2 + (z - z')^2})$ .

Instantiation of general formula (10) with the help of the  $z', \tau'$  plane diagrams (Fig. 2) reveals the explicit structure of the solution,

$$\text{if } -\infty < z < z_c \Leftrightarrow \tau_t > r,$$

$$\psi = \begin{cases} 0 & -\infty < \tau < r \\ \frac{\mu_0}{4\pi} ce\beta \int_0^{z_2} dz' \frac{f(\beta(\tau - r') - z')}{r'} & r < \tau < \infty \end{cases} \quad (11)$$

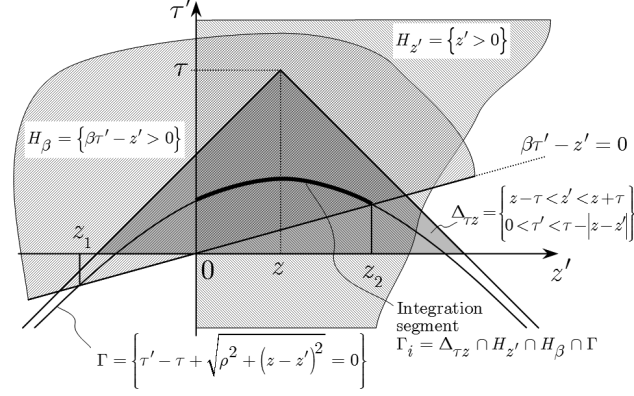


FIG. 1: Integration path for general solution (10).

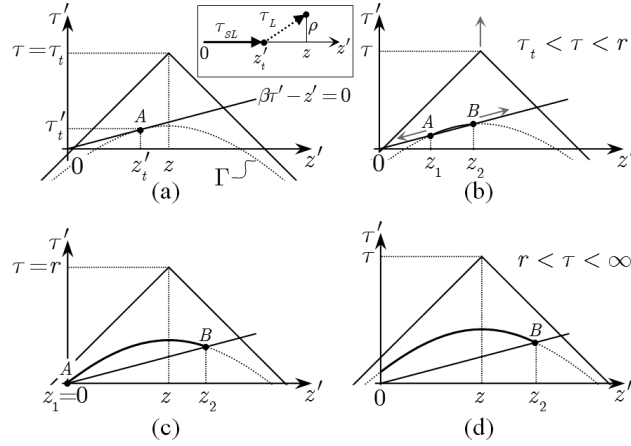


FIG. 2: Instantiation of general solution for the observation point  $\rho, z$ , case  $z > z_c$ .

otherwise ( $z_c < z < \infty \Leftrightarrow \tau_t < r$ )

$$\psi = \begin{cases} 0 & -\infty < \tau < \tau_t \\ \frac{\mu_0}{4\pi} c e \beta \int_{z_1}^{z_2} dz' \frac{f(\beta(\tau - r') - z')}{r'} & \tau_t < \tau < r \\ \frac{\mu_0}{4\pi} c e \beta \int_0^{z_2} dz' \frac{f(\beta(\tau - r') - z')}{r'} & r < \tau < \infty \end{cases} \quad (12)$$

that depends on the following parameters:  $z_{1,2} = \beta\gamma^2 \left[ \beta z - \tau \mp \sqrt{(\beta\tau - z)^2 - (\beta^2 - 1)\rho^2} \right]$ ,  $z_c = \gamma\rho$ ,  $\gamma = (\beta^2 - 1)^{-1/2}$ ,  $\tau_t = (z + \rho/\gamma)/\beta$ ,  $r = \sqrt{\rho^2 + z^2}$ , and  $r' = \sqrt{\rho^2 + (z - z')^2}$ . The result illustrates capability of the method – that does not resort to *a priori* causality conditions like retarded nature of the argument, wave propagation in a fixed direction, etc. – to yield solutions whose space-time structure admits easy *posterior* interpretation in terms of causal propagation of information:

For an observation point  $\rho, z$  there is no intersection between  $H_\beta$  and  $\Gamma$  (no wave registered) until the moment  $\tau = \tau_t$ , in which the hyperbola touches the boundary of  $H_\beta$  in the (tangency) point  $\tau'_t = (z - \gamma\rho)/\beta$ ,  $z'_t = z - \gamma\rho$ , as depicted in Fig. 2(a). For  $z > z_c$  the value of  $\tau_t = \tau_{SL} + \tau_L$  represents the minimum time necessary for the electromagnetic energy, originated in the space-time point  $\tau' = \rho' = z' = 0$ , to reach the observation point  $\rho' = \rho$ ,  $z' = z$  – first propagating during time  $\tau_{SL} = \tau'_t = (z - \gamma\rho)/\beta$  along the  $z'$  axis at the superluminal speed  $c\beta$  with the source-pulse front and then during time  $\tau_L = \sqrt{\rho^2 + (z - z'_t)^2} = \beta\gamma\rho$  out of this axis toward  $\rho, z$  at the luminal speed with the front of the emanated electromagnetic wave (see the upper diagram of Fig. 2(a)).

For cases corresponding to Figs. 2(a,b), Eq. (12) characterizes quantitatively a source pulse that appears to the observer "suddenly growing out of a point"  $z'_t, \tau'_t$  at  $\tau = \tau_t$  and expanding in the opposite directions, just as was predicted by Gron [1] on the basis of purely geometrical consideration (see also Fig. 15 of [4] or Fig. 1 of [30]). Notably, apart from [1], other pioneering papers showed how a superluminal source, after having suddenly revealed in an "optical-boom" phase, may subsequently appear as a couple of objects receding one from the other, in particular, in astrophysical observations (so-called "superluminal expansions"). For a detailed discussion of these models, both "orthodox" — in which a superluminal pattern is created by a coordinated motion of the subluminally moving constituents — and "true superluminal" — in which actual superluminal motions are treated within the framework of the extended special relativity theory —, the interested reader is directed to Recami et al. [31] and references therein.

Causal solution (12) demonstrates other phenomena discussed in the literature from the standpoint of the extended special relativity: as expound in [4], the superluminal (tachyonic) motions are always observed being forward in time, but can appear reversed in direction; as well, the duality between the source and detector makes possible the emission to be observed as absorption. In the case in question, the "post-boom" evolution of the source pulse is observed as forward and backward expansion. The latter stops as the pulse reaches its origin  $z' = 0$  (Figs. 2(c,d)) and at this point the (apparently reversed) generation process manifests as the pulse absorption. In the limiting case of a  $\delta$ -pulse the half-plane  $H_\beta$  degenerates into a line and the segment of integration  $\Gamma_i$  into points  $A$  and  $B$ , representing two images of the same tachyon. Source  $A$  is eventually absorbed at  $z' = 0$ , abruptly diminishing the wave amplitude (as will be shown later, by half).

The  $z, \tau$  plane map of the three areas differing in the solution representation is shown in Fig. 3. Aiming at construction of the propagation-invariant waves, it is worthwhile to express the wavefunction in terms of the propagation variable  $\xi = \beta\tau - z$ . In contrast to the pure steady-state solutions, representation of wavefront-limited causal waves does not exclude the time dependence,

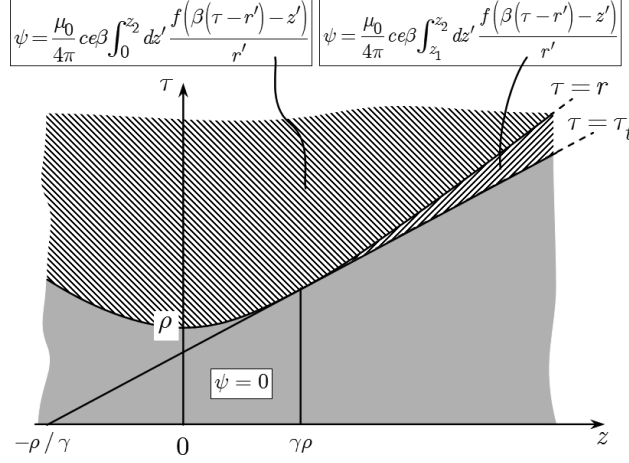


FIG. 3: Areas of case representation of  $\psi(\tau, \rho, z)$ .

and passing from  $\tau, \rho, z$  to  $\tau, \rho, \xi$  transforms:

(i) the non-zero wave condition  $\tau > \tau_t$  into  $\rho < \gamma\xi$ , a causal analog of the condition  $\rho < \gamma|\zeta| = \gamma|\xi|$ , reported in ([15], Eq. (8)) for the steady-state electromagnetic field of a charged tachyon — in agreement with predictions expound by Recami et al. on the basis of the extended theory of special relativity (see [30], especially Fig. 4, as well as earlier works on superluminal Lorentz transformations [32, 33]);

(ii) the case-limiting condition  $\tau < r(\tau, \rho, \xi) = \sqrt{\rho^2 + (\beta\tau - \xi)^2}$ , into  $\tau_1 < \tau < \tau_2$ , where

$$\tau_{1,2} = \tau - z_{2,1}/\beta = \gamma^2 \left( \beta\xi \mp \sqrt{\xi^2 - (\beta^2 - 1)\rho^2} \right) \quad (13)$$

are two roots of the equation

$$\tau_{1,2} - r(\tau_{1,2}, \rho, \xi) = 0; \quad (14)$$

(iii) case formulas (11), (12) into

**Case**  $-\infty < \xi < \rho/\gamma$  or  $(\rho/\gamma < \xi < \infty$  and  $-\infty < \tau < \tau_1)$

$$\psi(\tau, \rho, \xi) = 0, \quad (15)$$

**Otherwise Case**  $\tau_1 < \tau < \tau_2$

$$\psi(\tau, \rho, \xi) = \frac{\mu_0}{4\pi} ce\beta^2 \int_{\tau_1}^{\tau} d\tau' \frac{f(\beta[\tau' - r(\tau', \rho, \xi)])}{r(\tau', \rho, \xi)}, \quad (16)$$

**Case**  $\tau_2 < \tau < \infty$

$$\psi(\tau, \rho, \xi) = \frac{\mu_0}{4\pi} ce\beta^2 \int_{\tau_1}^{\tau_2} d\tau' \frac{f(\beta[\tau' - r(\tau', \rho, \xi)])}{r(\tau', \rho, \xi)}; \quad (17)$$

(iv) the case map of Fig. 3 ( $z, \tau$  plane) *into* the case map represented in Fig. 4 ( $\xi, \tau$  plane).

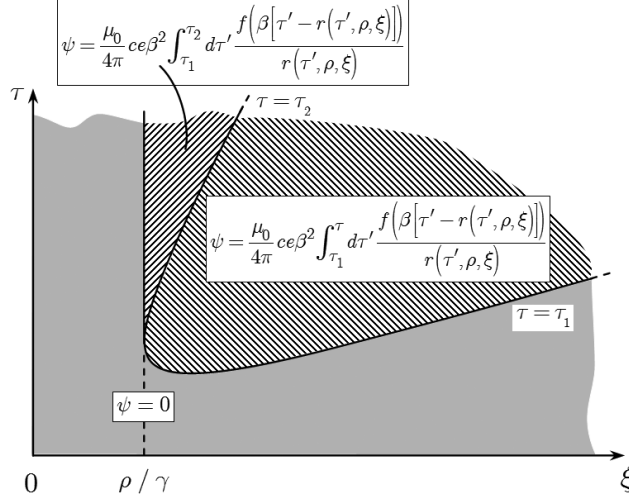


FIG. 4: Areas of case representation of  $\psi(\tau, \rho, \xi)$ .

Contour plot, representing the wave propagation via a characteristic space-time scale  $\lambda_0$  and the dimensionless quantities  $\tilde{\tau} = \tau/\lambda_0$ ,  $\tilde{\tau}_{1,2} = \tau_{1,2}/\lambda_0$ ,  $\tilde{\rho} = \rho/\lambda_0$ ,  $\tilde{\xi} = \xi/\lambda_0$ , is given in Fig. 5(a) ( $\beta = \sqrt{2}$ , as in numerical illustrations of Ref. [15]). For each fixed moment of time  $\tilde{\tau}$  the solid isoline  $\tilde{\tau}_1(\tilde{\rho}, \tilde{\xi}) = \tilde{\tau}$  defines the boundary of the wavefunction support (area  $\tilde{\tau}_1 < \tilde{\tau}$  corresponding to  $\psi \neq 0$ ) while the dashed isoline  $\tilde{\tau}_2(\tilde{\rho}, \tilde{\xi}) = \tilde{\tau}$  traces the boundary between cases (16) and (17). The emanated wave has an expanding droplet-shaped support, defined exclusively by the parameters  $\rho, \xi, \tau$ , and  $\beta$ . Fig. 5(b) represents the structure of this droplet-shaped wave for  $f(\xi) = \delta(\xi)$ ; the wavefunction is represented in dimensionless units via normalization  $\tilde{\psi} = \psi/\psi_0$ ,  $\psi_0 = \frac{\mu_0 c e}{2\pi \lambda_0}$ .

#### IV. DROPLET-SHAPED WAVES AS CAUSAL COUNTERPARTS OF THE X-SHAPED WAVES

Using the above approximation of an infinitely short source current pulse  $f(\xi) = \delta(\xi)$ , which in the case discussed in [15] led to the model of X wave generation by a charged tachyon, one readily arrives at the solution that in the area  $\xi > \rho/\gamma$  and  $\tau > \tau_1$  ( $\psi \neq 0$ ) reads

$$\psi = \begin{cases} \frac{\mu_0}{4\pi} c e \beta \int_{\tau_1}^{\tau} d\tau' \frac{\delta(\tau' - r(\tau', \rho, \xi))}{\tau'} & \tau_1 < \tau < \tau_2 \\ \frac{\mu_0}{4\pi} c e \beta \int_{\tau_1}^{\tau_2} d\tau' \frac{\delta(\tau' - r(\tau', \rho, \xi))}{\tau'} & \tau_2 < \tau < \infty. \end{cases} \quad (18)$$

The equation for the delta-function roots coincides with (14), so these roots,  $\tau' = \tau_{1,2}$ , are defined by formula (13). Using (9) and passing to the dimensionless parameters finally reduce (18) to the

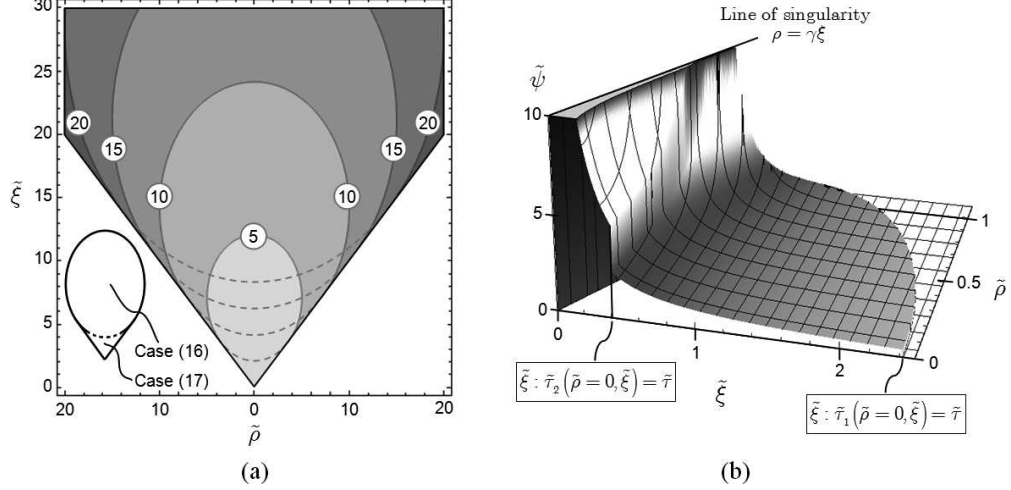


FIG. 5: (a) Contour plots illustrating the shape of the wavefunction support (solid isolines  $\tilde{\tau}_1 = \tilde{\tau}$ ) and the boundary between cases (16) and (17) (dashed isolines  $\tilde{\tau}_2 = \tilde{\tau}$ ); (b) a snapshot of  $\tilde{\psi}$ , clipped by  $\tilde{\psi} = 10$  in the vicinity of its singularities, taken at  $\tilde{\tau} = 1$ .

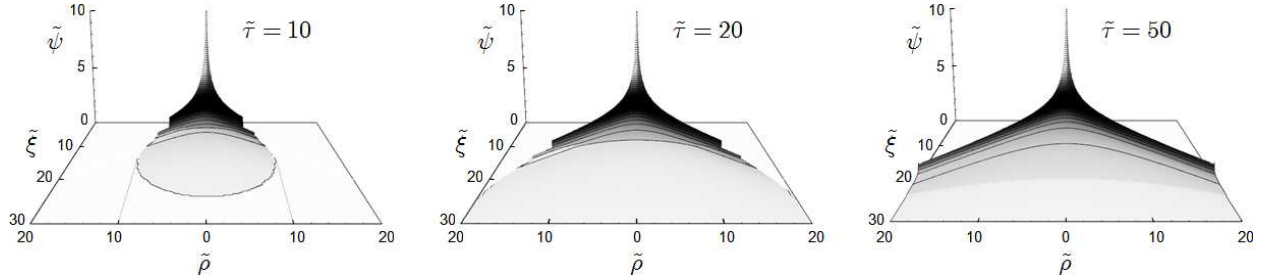


FIG. 6: Dynamics of the droplet-shaped wave propagation (the points on the vertex and the cone surface, in which  $\tilde{\psi}$  diverges, are omitted).

formula

$$\tilde{\psi}(\tilde{\tau}, \tilde{\rho}, \tilde{\xi}) = \begin{cases} \frac{1}{2} \frac{\beta}{\sqrt{\tilde{\xi}^2 - (\beta^2 - 1)\tilde{\rho}^2}} & \tilde{\tau}_1 < \tilde{\tau} < \tilde{\tau}_2 \\ \frac{\beta}{\sqrt{\tilde{\xi}^2 - (\beta^2 - 1)\tilde{\rho}^2}} & \tilde{\tau}_2 < \tilde{\tau} < \infty. \end{cases} \quad (19)$$

One can check by direct calculation that the second case of (19) corresponds to solution of the inhomogeneous wave equation of Ref. [15], describing the steady-state X wave produced by a charged tachyon (delta-pulse source). Introduction of the initial moment of particle generation results in launching of the same propagation-invariant waveform, which however is restricted by the droplet-shaped support illustrated in Fig. 5(a). As the time increases, this waveform expands in both  $\tilde{\rho}$  and  $\tilde{\xi}$  directions, tending to the charged-tachyon X-shaped field, as illustrated in Fig. 6. For  $\tilde{\tau}_1 < \tilde{\tau} < \tilde{\tau}_2$  the singularity corresponding to  $\tilde{\tau}_2$  (in Fig. 2, to  $z_1$ ) resides outside the integration

segment  $\Gamma_i$ , diminishing  $\psi$  by half.

Corresponding electromagnetic field vectors  $\mathbf{E} = -c(\nabla A^{(0)} + \partial\mathbf{A}/\partial\tau)$  and  $\mathbf{B} = \nabla \times \mathbf{A}$  (of which only  $E_\rho$ ,  $E_z$ , and  $B_\varphi$  components are nonzero), can readily be found using Eqs. (5) and (6). In particular, for the observation times  $\tilde{\tau} > \tilde{\tau}_2$  (a steady-state wave zone located outside the singularities arising from the potential discontinuities on the case delimiting boundaries of Fig. 4) the magnetic field (normalized by  $\psi_0\lambda_0^{-1}$ ) is characterized by  $\tilde{B}_\varphi = -\partial\tilde{\psi}/\partial\tilde{\rho} = -\tilde{\rho}\beta(\beta^2 - 1) [\tilde{\xi}^2 - (\beta^2 - 1)\tilde{\rho}^2]^{-3/2}$ . As in the case described in [15], Sec. III, it remains the only component that does not vanish when  $\beta \rightarrow \infty$ , revealing a "magnetic monopole" behavior. As put forward in [4, 30, 32, 33], the reference frame in which the particle velocity tends to infinity plays for tachyons the same role as the rest frame for ordinary particles (bradyons), and there exists a duality between subluminal electric charges and superluminal magnetic monopoles. So, for  $\beta \rightarrow \infty$  one might expect the magnetic field to have a structure akin to that of the electric field of a charged particle. Notably, earlier applications of the proposed technique to the waves emanated by subluminal sources (see, for instance, [28, 34]) result in peak- or ball-like shapes akin to the subluminal wave bullets obtained in Secs. II-IV of Ref. [35]. While electromagnetic fields of different line currents propagating at luminal speed present singularity at one "point of accumulation",  $\xi \equiv \tau - z = 0, \rho = 0$  (see, e.g., Fig. 1 of [36]), for the superluminal delta current the area of singularity spreads along the conical surface  $\xi - \rho/\gamma = 0$ , representing, according to [4, 30] an initially point-like structure (perceived by superluminal observers) highly distorted by the superluminal Lorentz transformation. In toto, the results obtained support the general idea about the shape of superluminal particles and distribution of the field associated with superluminal charges: "while the simplest subluminal object is obviously a sphere or, in the limit, a space point, the simplest superluminal object is on the contrary an X-shaped pulse" [35].

## V. CONCLUSION

The present work introduces a new type of the propagation-invariant, localized droplet-shaped waves that, being solutions of the inhomogeneous wave equation and satisfying zero initial conditions, admit causal generation by real pulsed superluminal sources widely discussed in the literature (see in particular the monograph [3] and more recent review [37] by Recami). Although the presented analysis is limited to the most illustrative case of  $\delta$ -pulse current, the general integral solution (15)-(17) enables the propagation-invariant localized droplet-shaped waves emanated by various line sources to be investigated both analytically and numerically using the  $z', \tau'$  diagrams similar to one

of Fig. 2. Various possible ansätze are discussed in [28] for free space and [38] for waveguides.

### Acknowledgements

The author is grateful to Michel Zamboni-Rached and Erasmo Recami for several useful discussions that significantly improved the introductory part of the article as well as for their kind cooperation that stimulated publication of this study. The research was partially based on work supported by the International Science Foundation under Grant M3H000 *Generation and Propagation of Localized Waves*.

- 
- [1] O. Gron, "Visual appearance of superluminal bodies," *Lett. Nuovo Cimento* **23**, 97–100 (1978).
  - [2] H. Lemke, "Light from sources moving faster than light," *Lett. Nuovo Cimento* **12**, 342–346 (1975).
  - [3] E. Recami, *Tachyons, Monopoles and Related Topics* (Elsevier, 1978).
  - [4] E. Recami, "Classical tachyons and possible applications," *La Rivista del Nuovo Cimento Series 3* **9**, 1–178 (1986).
  - [5] H. E. Hernández-Figueroa, M. Zamboni-Rached, and E. Recami, eds., *Localized Waves*, (Wiley, 2008).
  - [6] E. Recami, M. Zamboni-Rached, K. Z. Nobrega, C. A. Dartora, and H. E. Hernandez F., "On the localized superluminal solutions to the Maxwell equations," *IEEE Journal of Selected Topics in Quantum Electronics*, **9**, 59-73 (2003).
  - [7] D. Abdollahpour, S. Suntsov, D. G. Papazoglou, and S. Tzortzakis, "Spatiotemporal Airy light bullets in the linear and nonlinear regimes," *Phys. Rev. Lett.* **105**, 253901 (2010).
  - [8] E. Arévalo, "Boosted X waves in nonlinear optical systems," *Phys. Rev. Lett.* **104**, 023902 (2010).
  - [9] P. Saari and K. Reivelt, "Evidence of X-shaped propagation-invariant localized light waves," *Phys. Rev. Lett.* **79** 4135–4138 (1997).
  - [10] I. M. Besieris, M. Abdel-Rahman, A. M. Shaarawi, and A. Chatzipetros, "Two fundamental representations of localized pulse solutions to the scalar wave equation," *Prog. Electromagn. Res.* **19**, 1–48 (1998).
  - [11] P. Saari and K. Reivelt, "Generation and classification of localized waves by Lorentz transformations in Fourier space," *Phys. Rev. E* **69**, 036612 (2004).
  - [12] J. Salo, J. Fagerholm, A. Friberg, and M. Salomaa, "Unified description of nondiffracting X and Y waves," *Phys. Rev. E* **62**, 4261–4275 (2000).
  - [13] P. Di Trapani, G. Valiulis, A. Piskarskas, O. Jedrkiewicz, J. Trull, C. Conti, and S. Trillo, "Spontaneously generated X-shaped light bullets," *Phys. Rev. Lett.* **91**, 093904 (2003).
  - [14] M. A. Porras and P. Di Trapani, "Localized and stationary light wave modes in dispersive media," *Phys. Rev. E* **69**, 066606 (2004).

- [15] E. Recami, M. Zamboni-Rached, and C. A. Dartora, "Localized X-shaped field generated by a superluminal electric charge," *Phys. Rev. E* **69**, 027602 (2004).
- [16] S. C. Walker and W. A. Kuperman, "Cherenkov-Vavilov formulation of X waves," *Phys. Rev. Lett.* **99**, 244802 (2007).
- [17] M. Zamboni-Rached, "Unidirectional decomposition method for obtaining exact localized wave solutions totally free of backward components," *Phys. Rev. A* **79**, 013816 (2009).
- [18] M. Zamboni-Rached, E. Recami, and I. M. Besieris, "Cherenkov radiation versus X-shaped localized waves," *J. Opt. Soc. Am. A* **27**, 928–934 (2010).
- [19] I. M. Besieris, A. M. Shaarawi, and A. M. Attiya, "Bateman conformal transformations within the framework of the bidirectional spectral representation," *Prog. Electromagn. Res.* **48**, 201–231 (2004).
- [20] A. B. Utkin, "Mathieu progressive waves," *Commun. Theor. Phys.* **56**, 733–739 (2011).
- [21] R. W. Ziolkowski, I. M. Besieris, and A. M. Shaarawi, "Aperture realizations of exact solutions to homogeneous-wave equations," *J. Opt. Soc. Am. A* **10**, 75–87 (1993).
- [22] P. Saari, "Superluminal localized waves of electromagnetic field in vacuo," in D. Mugnai, A. Ranfagni, and L. S. Shulman, eds., *Time Arrows, Quantum Measurement and Superluminal Behaviour* (CNR, 2001), pp. 37–48 (arXiv:physics/0103054v1).
- [23] C. J. R. Sheppard and S. Saghafi, "Beam modes beyond the paraxial approximation: A scalar treatment," *Phys. Rev. A* **57**, 2971–2979 (1998).
- [24] D. Burgarella, M. Livio, and C. P. O’Dea, *Astrophysical Jets: Proceedings of the Astrophysical Jets Meeting, Baltimore, 1992 May 12-14* (Cambridge Univ. Press, 1993).
- [25] J. Vieira, S. Martins, V. Pathak, R. Fonseca, W. Mori, and L. Silva, "Magnetic Control of Particle Injection in Plasma Based Accelerators," *Physical Review Letters* **106**, 225001 (2011).
- [26] R. Courant and D. Hilbert, *Methods of Mathematical Physics, Vol. 2* (Wiley, 1989).
- [27] V. I. Smirnov, *Course of Higher Mathematics, Vol. 4, Part 2* (Pergamon, 1964).
- [28] A. B. Utkin, "Electromagnetic waves generated by line current pulses," in *Wave Propagation*, A. Petrin, ed. (InTech, 2011), pp. 483–508.
- [29] G. B. Arfken and H. J. Weber, *Mathematical Methods for Physicists* (Academic, 2001).
- [30] A. O. Barut, G. D. Maccarrone, and E. Recami, "On the shape of tachyons," *Il Nuovo Cimento A* **71**, 509–533 (1982).
- [31] E. Recami, A. Castellino, G. D. Maccarrone, and M. Rodonò, "Considerations about the apparent « superluminal expansions » observed in astrophysics," *Nuovo Cimento B* **93**, 119–144 (1986).
- [32] E. Recami and G. D. Maccarrone, "Solving the « imaginary quantities » problem in superluminal Lorentz transformations," *Lett. Nuovo Cimento Series 2* **28**, 151–157 (1980).
- [33] P. Caldirola, G. D. Maccarrone, and E. Recami, "Second contribution on solving the « imaginary quantities » problem in superluminal Lorentz transformations," *Lett. Nuovo Cimento Series 2* **29**, 241–250 (1980).
- [34] V. V. Borisov and A. B. Utkin, "The transient electromagnetic field produced by a moving pulse of

- line current," J. Phys. D **28**, 614–622 (1995).
- [35] M. Zamboni-Rached and E. Recami, "Subluminal wave bullets: Exact localized subluminal solutions to the wave equations," Physical Review A **77**, 033824 (2008).
- [36] V. V. Borisov and A. B. Utkin, "Some solutions of the wave and Maxwell's equations," J. Math. Phys. **35**, 3624 (1994).
- [37] E. Recami, "Superluminal motions? A bird's-eye view of the experimental situation," Found. Phys. **31**, 1119–1135 (2001).
- [38] A. B. Utkin, "Riemann-Volterra time-domain technique for waveguides: a case study for elliptic geometry," Wave Motion, to be published, doi:10.1016/j.wavemoti.2011.12.001, <http://www.sciencedirect.com/science/article/pii/S0165212511001430>